Optical and electronic properties of doped silicon from 0.1 to 2 THz

Martin van Exter and D. Grischkowsky
IBM Watson Research Center, P.O. Box 218, Yorktown Heights, New York 10598

(Received 11 December 1989; accepted for publication 14 February 1990)

Using a source of freely propagating subpicosecond pulses of THz radiation, we have measured the absorption and dispersion of both *N*- and *P*-type, 1 Ω cm silicon from 0.1 to 2 THz. These results give the corresponding frequency-dependent complex conductance over the widest frequency range to date. The data provide a complete view on the dynamics of both electrons and holes and are well fit by the simple Drude relationship.

The dynamics of carriers in semiconductors is important from both the scientific as well as the technical point of view. The most interesting phenomena occur at frequencies comparable to either the plasma frequency or the damping rate.[1-7] Unfortunately, this usually occurs in the submillimeter region, which is difficult to reach with microwave[2,6] as well as with far-infrared[1,7] techniques. Below 100 GHz, microwave techniques have been used for single-frequency studies. The high-frequency behavior of semiconductors has been investigated with classical far-infrared spectroscopy.[1,4,7] However, for moderate doping, the strongest absorption of the free carriers lies below 2 THz, where classical far-infrared spectroscopy becomes very difficult. Consequently, the investigation of the most important frequency range from 0.1 to 2 THz has remained incomplete (1.5 THz = 50 cm^{-1} = 6.2 meV).

Recently a new system has become available for spectroscopic studies in the range from 0.1 to 2.0 THz.[8,9] This system is based on the optoelectronic generation and reception of a beam of subpicosecond THz pulses. By inserting a sample in the beam and comparing the shape of the original subpicosecond THz pulses with the shapes of pulses that have propagated through the sample, one is able to deduce the frequency-dependent absorption and dispersion.

In this letter we describe an application of the above time-domain spectroscopy technique to a complete measurement of the absorption and dispersion due to carriers in doped silicon. The measured samples were *N*- and P-doped, 1 Ω cm silicon. The dopants were phosphorus and boron, respectively, and the flat wafers had a (111) orientation. The frequency-dependent properties are shown to be completely due to the carriers and not to the host crystal. Our measurements extend from 0.1 to 2 THz and allow for the most comprehensive determination of the complex conductivity to date. To first order the results are well fit by the simple Drude theory, although slight deviations indicate that further refinements in the theory are needed.

The setup used to generate and detect the short pulses of THz radiation is depicted in Fig. 1(a) and has been described earlier.[8,9] The transmitter and receiver are identical, each consisting of a micron-sized dipole antenna imbedded in a coplanar transmission line and optoelectronically driven by 70 fs pulses from a colliding-pulse mode-locked dye laser. A large fraction of the generated pulses of THz radiation is captured by a silicon lens attached to the transmitting chip and is directed onto a paraboloidal mirror that recollimates the radiation into a low divergence beam. This THz beam is directed towards the receiver where it is focused onto the receiving antenna. The amplitude and time dependence of the transient voltage induced across the receiving antenna are obtained by measuring the collected charge (current) versus the time delay between the THz pulses and the laser pulses that synchronously gate the receiver. Such a measured transmitted THz pulse with no sample in place is shown in Fig. 1(b). The corresponding amplitude spectrum of this 0.5 ps full width at half maximum pulse is presented in Fig. 1(c) and illustrates the 2 THz bandwidth available for spectroscopy.

Figure 2(a) shows a THz pulse transmitted through a 283-μm-thick sample of 1.15 Ω cm, *N*-type silicon. The first

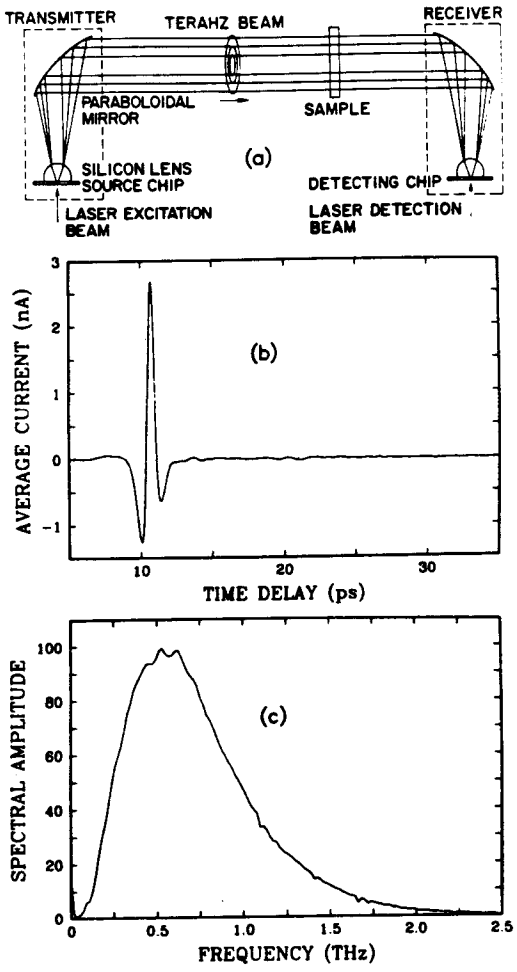

FIG. 1 (a) Schematic of the experiment; (b) measured transmitted THz pulse; (c) amplitude spectrum of (b).

 0003-6951/90/171694-03$02.00

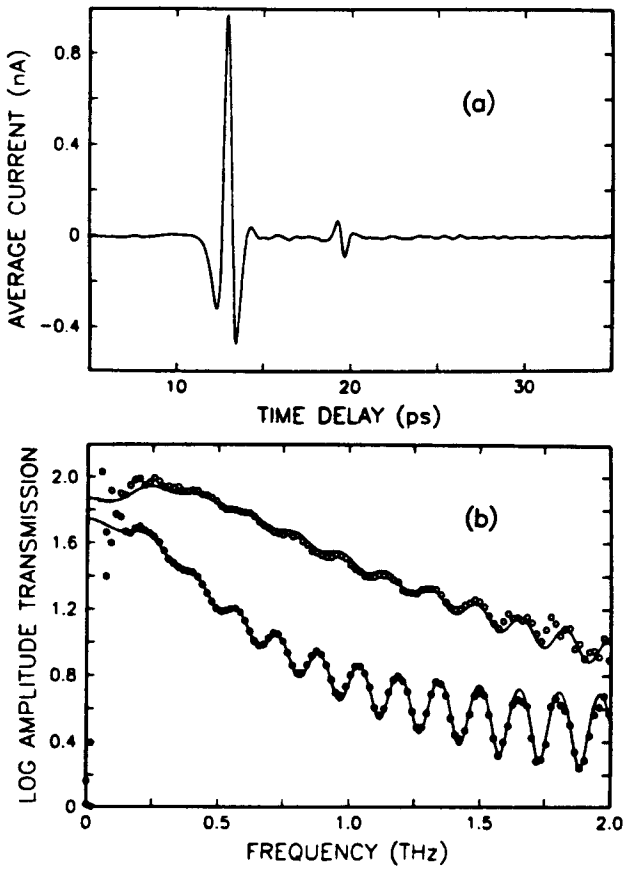

FIG. 2. (a) THz pulse transmitted through a 283-μm-thick wafer of 1.15 Ω cm, N-type silicon. (b) Logarithm of the amplitude transmission for a 283-μm-thick wafer of 1.15 Ω cm, N-type silicon (dots) and for a 258-μm-thick wafer of 0.92 Ω cm, P-type silicon (circles).

transient is the primary pulse that passed directly through the sample. Its peak amplitude is about 40% of that of the original pulse. The output pulse amplitude and shape are changed due to reflection losses, and the frequency-dependent absorption and dispersion of the sample. The second and barely resolvable third transients are THz pulses reflected inside the thin sample. Comparison of the Fourier transform of the single input pulse with that of the output pulse sequence from the doped silicon sample yields the frequency-dependent transmission plotted as $-\ln[(E_{\rm out}(\omega)/E_{\rm in}(\omega)]$ by the dots in Fig. 2(b). The open circles are measurements on a 258-μm-thick P-type sample that had a resistivity of 0.92 Ω cm. The multiple reflections are responsible for the oscillations in the frequency-dependent transmission of the sample. Similar oscillations are observed in the effective index of refraction, obtained by division of the phase shift of the transmitted spectral components by the length of the sample.

In order to quantitatively explain the above measurements, the index of refraction and absorption for undoped silicon was needed from 0.1 to 2.0 THz. Using time-domain spectroscopy, we have measured these quantities with high precision for a 20-mm-thick piece of float-zone-refined high-resistivity (10 kΩ cm) silicon. The index was found to be 3.415(2) and essentially constant over the entire frequency range, being in good agreement with the literature value of 3.416 at 1.0 THz.[10] The high-resistivity silicon was almost transparent over the entire frequency range, with a measured intensity absorption of <0.04 cm^{-1}. Consequently, the observed strong frequency dependence for doped silicon is due to the carriers and not to the host crystal.

The Drude model[5-7] treats the free carriers in a solid as classical point charges subject to random collisions. In this letter the simplest versus of the Drude model is adopted, in which the collision damping is independent of the carrier energy. According to the Drude model, the frequency-dependent complex dielectric constant ϵ, being the square of the complex index of refraction $n = n_r + {\rm i}n_i$, in SI units is

$$\epsilon = \epsilon_\infty + i\sigma/\omega\epsilon_0 = \epsilon_\infty - \omega_p^2/\omega(\omega + i\Gamma),$$
$$\sigma = \sigma_{\rm dc} i\Gamma/(\omega + i\Gamma) = i\epsilon_\infty\omega_p^2/(\omega + i\Gamma),$$

where ϵ_∞ is the contribution of the bound electrons, $\Gamma = 1/\tau$ is the damping rate, and τ is the average collision time. The plasma angular frequency ω_p is defined by $\omega_p^2 = Ne^2/\epsilon_0 m$, where N is the number density of carriers, e is the electronic charge, ϵ_0 is the free-space permittivity, and m is the effective carrier mass. We have also presented the Drude result for the complex electric conductivity σ, where the dc conductivity $\sigma_{\rm dc}$ is given by $\sigma_{\rm dc} = e\mu N$ with the mobility μ given by $\mu = e/m\Gamma$. The experimentally determined transmission is related to the above equations via the intensity absorption coefficient α, usually specified in cm^{-1}, which is $\alpha = n_i(4\pi/\lambda_0)$.

To include the effects of multiple reflections we fit the measurements with a model for the transmission through a reflective, lossy parallel slab of material with frequency-dependent optical properties described by the Drude model. The solid lines in Fig. 2(b) are theoretical fits. From the experimental data, both Drude parameters, the plasma angular frequency ω_p and the damping rate Γ, could be determined within 5% accuracy. For 0.92 Ω cm P-type silicon we found $\omega_p/2\pi = 1.75$ THz and $\Gamma/2\pi = 1.51$ THz, while for 1.15 Ω cm N-type silicon $\omega_p/2\pi = 1.01$ THz and $\Gamma/2\pi = 0.64$ THz. The measurements immediately show the different dynamic behavior of the electrons and the holes. For our situation of moderate doping and room temperature the damping rate Γ is mainly determined by carrier-phonon collisions,[2,4,11] a process that apparently is more efficient for holes than for electrons. A combination of the measured damping rates and the effective carrier masses, which have been measured to be $0.26m_0$ for the electrons and $0.37m_0$ on the average for the light and heavy holes,[1,12,13] where m_0 is the free-electron mass, yield mobilities of 1680 cm^2 V^{-1} s^{-1} for the electrons and 500 cm^2 V^{-1} s^{-1} for the holes. These values are higher than the literature values of 1400 and 400 expected for the doping levels of the N- and P-type silicon, respectively.[12,14] This disagreement may indicate the need for an extension of the simple Drude model; for example, many sophisticated models have been developed,[2,4,11] separating the carrier relaxation into both inter- and intravalley scattering with (acoustic and optic) phonons and with ionized impurities.

The second fit parameter, the plasma frequency, is proportional to the root of the ratio of the carrier density over the effective mass. The difference in plasma frequency between P- and N-type material mainly reflects the larger

doping needed in the *P*-type to compensate for the higher damping rate and to get the same dc conductivity. Combining the measured plasma frequencies with the respective effective carrier masses, we calculated a carrier density of $1.4\times10^{16}\,\mathrm{cm}^{-3}$ for the *P*-type and $3.3\times10^{15}\,\mathrm{cm}^{-3}$ for the *N*-type silicon. This is rather low compared to the doping levels of $1.8\times10^{16}\,\mathrm{cm}^{-3}$ and $4.6\times10^{15}\,\mathrm{cm}^{-3}$ specified by the manufacturer to $\pm 20\%$.

To facilitate interpretation of the data we removed the influence of reflections numerically, using the dielectric function obtained from the Drude fit. The correction, of which the result is shown in Fig. 3(a), is especially important for the very high frequencies, where the absorption is low and the interference fringes are strong, and for the very low frequencies, where the index of refraction becomes large. The absorption is seen to be quite strong, more than 2000 times greater than that of the host crystal. Below 0.15 THz the data become noisy due to the limited beam power, but the theoretically predicted drop in absorption at low frequencies is clearly observable. In Fig. 3(b), we present the obtained real part of the index of refraction versus frequency. This quantity is strongly frequency dependent, showing a clear minimum followed by a dramatic increase towards low frequencies. The agreement between this THz optical data and the simple Drude theory is exceptional.

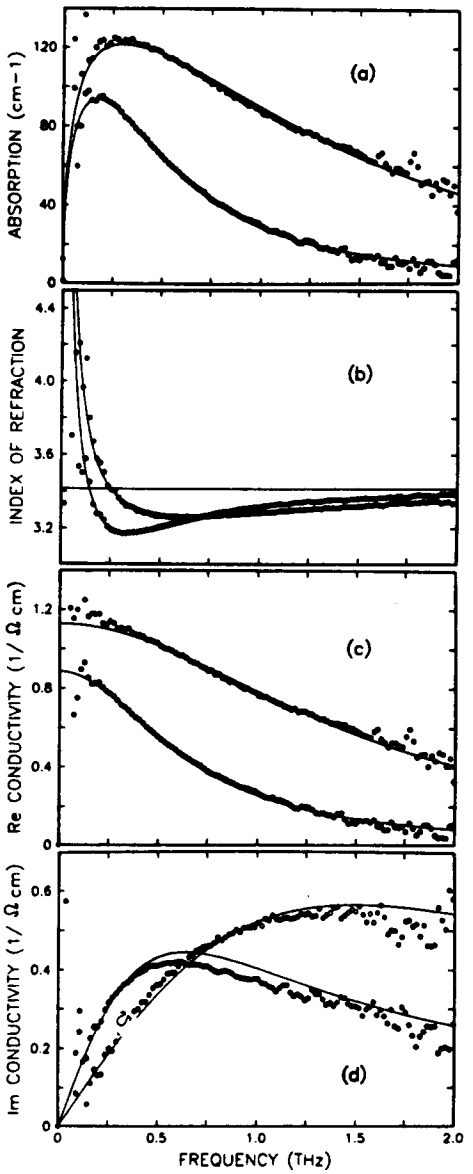

FIG. 3. Results for 1.15 Ω cm, *N*-type (dots) and 0.92 Ω cm, *P*-type (circles) silicon. (a) Intensity absorption calculated from the measured transmission of Fig. 2(b); (b) real part of the index of refraction; (c) real part of the electric conductivity; (d) imaginary part of the electric conductivity.

As the THz optical properties of the samples are largely determined by the carrier dynamics, we have indirectly measured the electric conductivity of the doped silicon. To link the optical measurements with electronics, the real part of the electric conductivity calculated from the optical data is shown in Fig. 3(c) and the imaginary part in Fig. 3(d). The real part is strongly frequency dependent, dropping monotonically from its dc peak to a reduced value at the highest measured frequency of 2 THz. The extrapolated dc conductivities are 0.89 Ω cm for the *P*-type material and 1.13 Ω cm for the *N* type, comparing favorably with the directly measured values of 0.92 Ω cm (*P* type) and 1.15 Ω cm (*N* type). The behavior of the imaginary part is completely different, increasing from zero at low frequencies, peaking at mid-range, and then showing a gradual decline. The agreement with the Drude theory of both the real and imaginary part of the conductivity is quite acceptable.

We acknowledge the excellent masks and wafer fabrication by Hoi Chan and the discussions with Søren Keiding. This research was partially supported by the U.S. Office of Naval Research.

[1]W. G. Spitzer and H. Y. Fan, Phys. Rev. **106**, 882 (1957).
[2]J. D. Holm and K. S. Champlin, J. Appl. Phys. **39**, 275 (1968).
[3]S. J. Allen Jr., D. C. Tsui, and F. DeRosa, Phys. Rev. Lett. **35**, 1359 (1975).
[4]M. Vindevoghel, J. Vindevoghel, and Y. Leroy, Infrared Phys. **15**, 161 (1975).
[5]N. W. Ashcroft and N. D. Mermin, *Solid State Physics* (Holt, Rinehart and Winston, New York, 1976).
[6]R. T. Kinasewitz and B. Senitzky, J. Appl. Phys. **54**, 3394 (1983).
[7]T. Ohba and S. Ikawa, J. Appl. Phys. **64**, 4141 (1988).
[8]M. van Exter, Ch. Fattinger, and D. Grischkowsky, Appl. Phys. Lett. **55**, 337 (1989).
[9]M. van Exter, Ch. Fattinger, and D. Grischkowsky, Opt Lett. **14**, 1128 (1989).
[10]E. V. Loewenstein, D. R. Smith, and R. L. Morgan, Appl. Opt. **12**, 398 (1973).
[11]P. A. Schumann Jr. and R. P. Phillips, Solid-State Electron. **10**, 943 (1967).
[12]S. M. Sze, *Physics of Semiconductor Devices* (Wiley, New York, 1981).
[13]R. N. Dexter, H. J. Zeiger, and B. Lax, Phys. Rev. **104**, 637 (1956).
[14]C. Jacoboni, C. Canali, G. Ottaviani, and A. Alberigi Quaranta, Solid-State Electron **20**, 77 (1977).